

Modeling of the Cs¹³⁷ and Sr⁹⁰ contamination transportation process performed for the vicinity of National Radioactive Wastes Disposal in Różan (NE Poland)

M. MIECZNIK¹, J.W. MIETELSKI¹, E. ŁOKAS¹, K. KLESZCZ²

magdalena.miecznik@ifj.edu.pl, jerzy.mietelski@ifj.edu.pl, edyta.lokas@ifj.edu.pl,
k_kleszcz@pwsztar.edu.pl

¹Institute of Nuclear Physics Polish Academy of Sciences, Radzikowskiego 152,
31-342 Krakow, Poland

²State Higher Vocational School in Tarnow, Poland, Mickiewicza 8, 33-100 Tarnow, Poland

This paper contains the results of radionuclides transportation modeling under National Radioactive Waste Disposal (NRWD) grounds in Różan (northeast Poland). The disposal is of the low- and intermediate-level waste (LILW) type. We simulated the radionuclides transportation process through sandy soils. The simulation was performed in a self-written simulator in Scilab using the finite difference method. The model included diffusion, advection and radioactive decay. The model was tested according to convergence and stability. Assuming the hydrological gradient being 0.008, the contamination transportation time was 30–46 years depending on the modeled problem. The modeled distance of 600 m was from underneath the disposal to the exudation in the Narew ravine. Radioactive decay for both cesium (Cs¹³⁷) and strontium (Sr⁹⁰) had a significant impact on the results. The model proved to be a useful tool for performing simple scientific simulations. This survey was part of a PhD thesis.

Keywords: advection, diffusion, radioactive decay.

DOI: 10.5604/01.3001.0012.2002

1. Introduction

The city of Różan is located about 90 km to the northeast of Warsaw. Since 1961, the old military fort in Różan has been used as the NRWD [1]. The military fort was built in 1905–1908. According to [2], the disposal spans 1.7 ha. The International Atomic Energy Agency (IAEA) classification specifies the disposal as a surface-type object for low- and intermediate-level waste (LILW) [8]. In this type of disposal, only radionuclides with a half-life ≤ 30 years (β - and γ - type) can be deposited. The long-life α -decay isotopes can be stored there only in limited amounts and for a limited time [9]. The disposal is about 800 m from Narew River. The fort was built on sandy soil, which is highly permeable. Nevertheless, selecting this structure as the NRWD was probably the best possible solution at that time.

The archaic construction of the fort, the vicinity of Narew River and the sandy base have led to the potential soil contamination becoming a very interesting research problem.

We modeled the contamination leakage in a self-written simulator.

2. Software and data availability section

The simulation was performed in Scilab 5.5.2 (64-bit). The computer parameters were: Intel Core i7-2600 CPU processor @ 3.40 GHz 3.70 GHz x64, 8.00 GB RAM, Windows 10 Pro.

Soil type was determined by geological and granulometric analysis of 7- and 8-m deep cores sampled about 100 m from the National Radioactive Waste Disposal (NRWD) in the direction of Narew River. Sand, clay and gravel were identified in the samples.

The diffusion coefficient was assumed to be 10^{-9} m²/s; advection velocity was calculated from hydraulic conductivity and assumed pressure difference. Hydraulic conductivity was calculated both as an average for all sand, clay and gravel content from table values and from the literature for this particular hydrogeological unit. Pressure difference depended on the modeled scenario.

3. Conceptual model

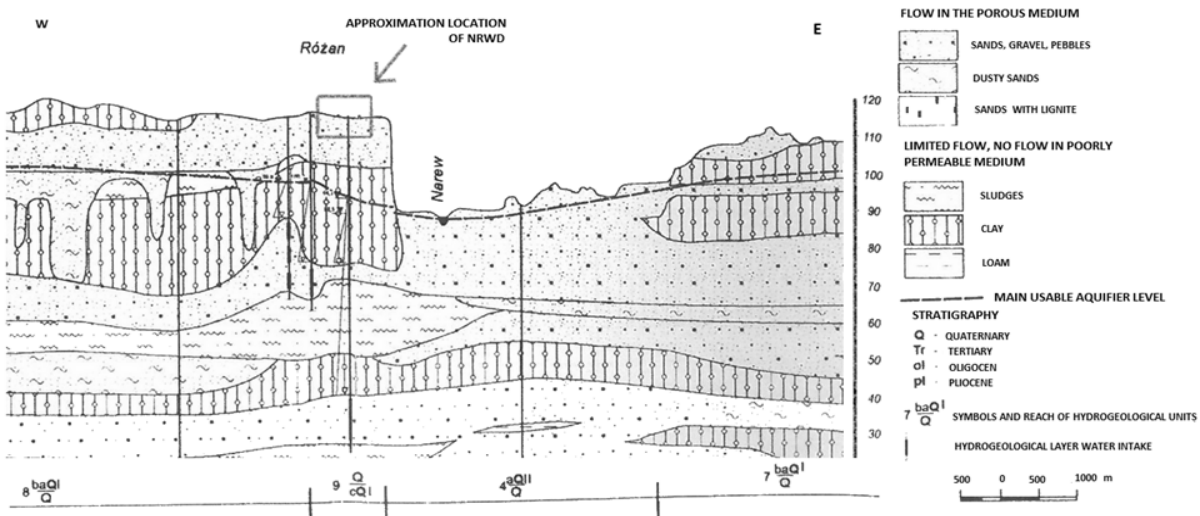


Fig. 1. Geological cross-section of modeled area [2]

The conceptual model was defined based on a geological cross-section (Figure 1) and two cores sampled about 100 m to the east of the NRWD (Narew River direction). The Różan NRWD is located on approximately 16–20 m dry sand, and there are several meters of hydrated sand and boulder clay reaching the Narew riverbed to the east. The Narew riverbed lies at an altitude of about 90 m above sea level; the disposal is about 115 m above sea level and the clay begins about 105 m above sea level [2].

This information aided the determination of the spatial model frames. The modeling area encompassed 600 m from the NRWD to the slope of the ravine on the west bank of Narew River, where exudation is expected. At this point, the clay layer changes into the sand layer. The vertical model dimension is 20 m, which is the depth under the disposal where the clay layer appears.

The modeling area was divided into two regions. The first region covered an area of dry sand assumed to be 16 m below the bottom of the disposal (this can change according to seasonal rain intensity). The second region covered a range of 4 m hydrated sands of up to 20-m deep and 600 m from the NRWD to Narew River. This 4-m region was qualified as the first aquifer [2]. These two regions yielded two connected 1-dimensional (1-D) models. The flow rate in the first region is driven by gravity but can also be counteracted by suction pressure [3] (related to absorption), adsorption or radioactive decay. The balance between hydrostatic pressures (gravity-driven flow) and suction pressure results from the saturation level

of the dry sands. For weakly loamy sands, field water capacity corresponding to a suction pressure of 100 cm (which corresponds to 100 hPa) is achieved for the saturation value $\theta = 20\%$ [3]. A saturation $\theta > 20\%$ indicates gravity-driven flow, while for $\theta \leq 20\%$, the water is retained in the ground until it exceeds 20%. The above considerations can be implemented into the Darcy equation (1) as shown below. Darcy law indicates that the flow is due to the pressure difference and has the following form:

$$\vec{w} = -\frac{K}{\mu} \nabla(p - \rho \vec{g} \vec{h}), \quad (1)$$

where:

\vec{w} is the liquid velocity through the porous medium,

K [m^2] permeability,

μ [$\text{Pa} \times \text{s}$] dynamic viscosity,

\vec{g} [m/s^2] gravity attraction,

\vec{h} [m] height,

ρ [kg/m^3] liquid density and p [Pa] pressure.

When there is no pressure difference, then there is free gravity flow (equation 2).

$$\vec{w}_f = \frac{K}{\mu} \rho \vec{g} \quad (2)$$

The \vec{w}_f is a filtration coefficient. When the only pressure is suction pressure, then the fluid velocity is calculated as below (equation 3):

$$\vec{w} = \vec{w}_f + \vec{w}_s = \vec{w}_f - \frac{K}{\mu} \nabla p = \vec{w}_f - \frac{\vec{w}_f * \mu}{\rho \vec{g}} * \rho \vec{g} \nabla F = \vec{w}_f - \vec{w}_f * \nabla F, \quad (3)$$

where:

w_s is a velocity resulting from the suction pressure and F [cm] the suction pressure expressed in the difference in the liquid column height.

Equation 3 indicates that the flow will not occur if $F = 1$ m, which corresponds to a weak loam sands field water capacity equal to 20% saturation. For F in the range of 0–1 m, water will flow according to gravity, but slower; for $F \leq 0$ m, water will flow freely according to gravity, and for $F > 1$ m, water will be retained in the soil pores. It follows that for irrigated sands, three options should be considered: $F \geq 1$ m, $F \in (1 \text{ m}, 0 \text{ m})$ and $F = 0$ m.

For the first case, absorption will be the process that will halt the spread of contamination beneath the landfill (analogous to a dry sponge retendering water). Assuming that the ground under the landfill is completely dry, then its absorption capacity would be equal to 20% of its volume, according to θ [3].

In the second case, the gravity flow will take precedence, but it will be slowed by the suction pressure. For the third situation, there will be free gravity flow.

In the case of the hydrated sand layer, within the first aquifer, flow will be determined by the pressure difference resulting from the difference in groundwater levels below the disposal and the exudation on the bank of Narew River. Then, equation 1 will be transformed as follows (4): where h [m] is height,

∇h a hydraulic gradient, Δh [m] the difference in ground water levels between the area underneath the disposal and the exudation on the Narew riverbank, and l [m] the distance between the abovementioned localizations without including tortuosity in porous connections.

The hydraulic gradient for the first aquifer can differ according to seasonal rain intensity.

$$\vec{w} = -\frac{K}{\mu} \nabla p = -\frac{K}{\mu} \rho \vec{g} \nabla h = -\frac{K}{\mu} \rho \vec{g} \frac{\Delta h}{l} \quad (4)$$

where:

h [m] is height,

∇h is a hydraulic gradient,

Δh [m] is the difference in a ground water levels between the place underneath the disposal and the exudation on the Narew river bank,

l [m] is the distance between mentioned localizations without including tortuosity in porous connections.

The hydraulic gradient for the first aquifer can differ according to seasonal rain intensity.

In the experiment that was part of the PhD thesis, the adsorption parameters for four layers of sediments from the 8-m deep core were explored. Based on granulometric analysis, the filtration coefficients for each layer were calculated to be about 5×10^{-5} m/s.

In the literature, the given filtration coefficient for the fine sands underneath the landfill is between 6×10^{-6} and 6×10^{-5} m/s [4]. The upper limit corresponds to the values calculated by the authors based on granulometric analysis. The diffusion coefficient was assumed to be 10^{-9} m²/s [3].

The flow through dry sands will be in the vertical direction and the flow through the aquifer will be in the horizontal direction. Therefore, the computer model was divided into two 1-D models. The initial condition for the system is a point source of contamination equal to 50 kBq/ml. The contamination distribution is driven by the diffusion resulting from the concentration difference and advection. The advection is driven by gravity or hydraulic gradient according to the vertical or horizontal model. The adsorption, if present, would counteract the contamination spread.

The preliminary analysis divided the second sampled core into four layers. During the PhD experiment, adsorption analysis was performed. Adsorption was also simulated in the computer model, but due to some numerical problems, the results were not valuable. The adsorption parameters in the model were set for the Langmuir isotherm from the experiment for the least-adsorbing layer. This was mainly because there is no exact knowledge of the kind of settlements below the level of 8 m, i.e. the depth of the second core. The model was divided into a grid of 16×3 knots for the “dry” sands layer (WN), and 3×60 knots for the irrigated sand (WW) layer. For the dry sands, the spatial step in the vertical direction (Δy) was 2 m, so it mapped the equivalent of 32-m depth. In the horizontal direction (Δx), the spatial step was also 2 m, but it was relevant only to the stability of the calculation and the resolution of the baseline on graphics, as both the diffusion coefficient and advection velocity in the x-direction were set as 0. In the case of the hydrated sands, a spatial step in the horizontal direction Δx was 20 m and that in the vertical direction Δy was 10 m. As was in the case of the dry sands, but for the y-direction, this step was important only because of the calculation stability and the baseline resolution in the graphic it mapped, which was equivalent to 1200 m of the horizontal model. For the hydrated sands, the advection velocity and diffusion coefficients were 0 in the y-direction. The whole model area was covered by the 16×3 grid in the dry sand model and by 3×60 m in the hydrated sand model. The numerical models were extended twice

their size in comparison to the conceptual models because this allowed us to retain all outflow data. If the model was set for 8×3 and 3×30 , then the boundary conditions could influence the outflow results. The computer model accuracy is strongly related to grid density. A denser grid indicates a longer calculation time. The spatial step, time step, advection velocity, initial value of contamination and distance from the source to the edges of the model influence the model convergence, stability and computation time. It is necessary to compromise between these model parameters. For dry sands, three simulations were performed: the first for suction pressure $F = 0.01$ m ($\theta \sim 42\%$, assuming the sand was wet), corresponding to free gravity flow [3] and the source of 50 kBq/ml with only diffusion and advection, the second had the same parameters as the first plus the radioactive decay for cesium (Cs), and the third was like the second but included strontium (Sr) decay instead of Cs decay. For the hydrated sands, we also performed three simulations: the first was for a groundwater level gradient of 0.008 (groundwater level difference $\Delta h = 5$; distance 600 m) with only advection and diffusion, the second was like the first but with radioactive decay for Cs, and the third was like the second but with radioactive decay for Sr instead of for Cs. The simulation results for the dry sands were set as input data to the hydrated sands model. In the presented simulator, it was also possible to implement a linear adsorption isotherm, but this approximation is only real for micro-concentrations [3] of the contaminant. The Langmuir isotherm was implemented to the code, but there were some numerical problems we could not solve.

4. Mathematical model

In the mathematical sense, the studied phenomenon can be described by three equations: the transportation equation 5 [5], the Darcy law equation 1 and radioactive decay law equation 6. The transportation equation here includes adsorption, advection and diffusion.

$$\frac{\partial}{\partial t} \left(C + \frac{\rho_b q}{p} \right) = -\frac{\partial}{\partial x} (\vec{w}C) + \frac{\partial}{\partial x} \left(D \frac{\partial C}{\partial x} \right) \quad (5)$$

$$C = -C_0 * \exp(-\lambda * t) \quad (6)$$

where:

C is the tracer concentration in the solution,
 C_0 the initial tracer concentration in the solution,
 λ a radioactive decay constant,

ρ_b the soil bulk density,

q the adsorption (the unit of adsorbed matter per unit of soil),

p the porosity,

\vec{w} the advection velocity,

D the diffusion coefficient.

The adsorption is described by the adsorption isotherm.

In this case, the Langmuir isotherm was used (equation 7).

$$\frac{\partial}{\partial t} \left(C + \frac{\rho_b \frac{abC}{1+bC}}{p} \right) = -\frac{\partial}{\partial x} (\vec{w}C) + \frac{\partial}{\partial x} \left(D \frac{\partial C}{\partial x} \right) \quad (7)$$

where

$$\left(1 + \frac{\rho_b \frac{ab}{1+bC}}{p} \right) = R$$

is the retardation factor.

$$t_q = R * t_m \quad \text{or} \quad w_q = R * w \quad (8)$$

Equations 8 means that the transportation time of the tracer is delayed according to solution transportation by the factor R. The same relation is valid for advection velocity [5]. In the model, the searched is a contamination expansion in the entire modeled area. In the model, there were Neumann boundary conditions. For the dry sands, both advection and diffusion coefficient for the top and side edges were defined as 0. For the hydrated sands, both advection velocity and diffusion coefficient for the top, bottom and left edges were defined as 0 as well.

5. The numerical model

In the form of a difference equation, the transportation equation that includes advection and diffusion but not adsorption can be expressed as follows (9):

$$\begin{aligned} \frac{C_{ij}^{k+1} - C_{ij}^k}{\Delta t} = & -w_y \frac{C_{i+1,j}^{k+1} - C_{i,j}^{k+1}}{\Delta y} - w_x \frac{C_{i,j+1}^{k+1} - C_{i,j}^{k+1}}{\Delta x} + \\ & + D_y \frac{C_{i-1,j}^{k+1} - 2 * C_{i,j}^{k+1} + C_{i+1,j}^{k+1}}{\Delta y^2} + D_x \frac{C_{i,j-1}^{k+1} - 2 * C_{i,j}^{k+1} + C_{i,j+1}^{k+1}}{\Delta x^2} \end{aligned} \quad (9)$$

In the above approximation of the transportation equation, the implicit approximation scheme was used. In this regard, the concentration value in the point i, j and time $k+1$ (C_{ij}^{k+1}) was calculated based on the adjacent points in the $k+1$ moment as well as from the already known C_{ij}^k . This approximation requires evaluating the system of the equations [6]. Below the transportation equation including adsorption was discretized starting with the left side of equation 7, 10 and 11 [7]:

$$\begin{aligned} L = \frac{\partial}{\partial t} \left(C + \frac{\rho_b \frac{abC}{1+bC}}{p} \right) & = \frac{\partial C}{\partial t} + \frac{\partial S}{\partial t} = \frac{\partial C}{\partial t} + \frac{\partial S}{\partial C} \frac{\partial C}{\partial t} = \\ & = \frac{\partial C}{\partial t} \left(1 + \frac{\partial S}{\partial C} \right) = \frac{\partial C}{\partial t} R(C) \end{aligned} \quad (10)$$

Equation 10 has been changed from a differential to difference equation 11:

$$\frac{\partial C}{\partial t} \left(1 + \frac{\partial S}{\partial C}\right) = \frac{\partial C}{\partial t} R(C) \rightarrow \frac{C_{ijl}^{k+1} - C_{ijl}^k}{\Delta t} \left[1 + \frac{\rho_b * a * b}{p} * \left(\frac{C_{ijk}^{l+1}}{1+b*C_{ijk}^{l+1}} - \frac{C_{ijk}^l}{1+b*C_{ijk}^l}\right) * \frac{1}{\Delta C}\right] \quad (11)$$

Indexes i, j, k, and l in equation 11 mean: i and j are spatial steps with Δx and Δy length, k a time step with Δt length and l a concentration step with ΔC length. Therefore, equation 7 can be expressed in the form of a difference equation as follows:

$$\begin{aligned} & \frac{C_{ijl}^{k+1} - C_{ijl}^k}{\Delta t} \left[1 + \frac{\rho_b * a * b}{p} * \left(\frac{C_{ijk}^{l+1}}{1+b*C_{ijk}^{l+1}} - \frac{C_{ijk}^l}{1+b*C_{ijk}^l}\right) * \right. \\ & \left. * \frac{1}{\Delta C}\right] = -W_y \frac{C_{i+1jl}^{k+1} - C_{ijl}^{k+1}}{\Delta y} - W_x \frac{C_{ij+1l}^{k+1} - C_{ijl}^{k+1}}{\Delta x} + \\ & + D_y \frac{C_{i-1jl}^{k+1} - 2*C_{ijl}^{k+1} + C_{i+1jl}^{k+1}}{\Delta y^2} + D_x \frac{C_{ij-1l}^{k+1} - 2*C_{ijl}^{k+1} + C_{ij+1l}^{k+1}}{\Delta x^2} \end{aligned} \quad (12)$$

The system of equations was built by writing the difference equation for each knot point. Initially, the matrix was constructed for a small grid and then according to recurrence was expanded into the planned size. Then, the parameters were grouped according to the element ($C_{i...j...l...}^{k+1}$) position in the matrix. The system of equations was calculated and results of the previous calculation were set as known to the next step. Based on the known value of C_{ijl}^k , the retardation factor $R_{ijl}^k(C)$ was calculated for each step for the assumed value of ΔC . Then, elements C_{ijl}^{k+1} and C_{ijl}^k were multiplied by the value of $R_{ijl}^k(C)$. For each time step, the matrix of known C_{ijl}^k was multiplied by the $\exp(-\lambda * \Delta t)$, yielding C_{ijl}^{k+1} (equation 13).

$$C_{ijl}^{k+1} = -C_{ijl}^k * \exp(-\lambda * \Delta t) \quad (13)$$

The initial condition for the dry sands model was the source equal to 50 kBq/ml in node (2,2) of the 16×3 grid. The 8×3 model was extended to 16×3 to retain information on the peak contamination spread when the maximum reached outflow [node (8,2)]. The second reason for the model extension was to test whether the sum of radionuclide concentration in all model knots when the maximum reached the outflow [node (8,2)] was convergent to the initial concentration.

For the hydrated sands, the modeled area was related to the 3×30 grid, but calculations were done for the 3×60 grid. The outflow from the dry sands was an inflow for the hydrated sands.

6. Testing model convergence and stability

The convergence and stability were tested by setting for all four edges Neumann boundary conditions with advection velocity and diffusion coefficient equal to 0 on these edges. Then, for an assumed number of time steps, the simulation was run assuming a different time step each time, as spatial steps had already been defined according to the model geometry. At the end, the contaminant concentration in all model nodes was summed and divided by the source defined in the initial conditions.

The chosen parameters yielded error not greater than 0.1%. The following parameters were set for the dry sands (WN) and the hydrated sands (WW): $S = 50000$ Bq/ml, $\Delta t = 50$ s; and $S = 50000$ Bq/ml, $\Delta t = 500000$ s, respectively. As numerical problems, calculations in practice do not include adsorption. For Cs^{137} , the adsorption isotherm parameters were 580 Bq/g and 0.0035 ml/Bq. This as well as the adsorption parameters for Sr^{90} were found in the first experimental part of the PhD research. In the case of Cs^{137} , it was necessary to use $\Delta C = 30000$ Bq/ml; otherwise, the model would not be convergent. On the other hand, using a big concentration step caused the loss of information on the adsorption. It stemmed from the fact that derivative $\frac{\partial S}{\partial C}$ from equation 10 for $C \rightarrow \infty$ goes to 0 (equation 14).

$$\lim_{C \rightarrow \infty} \frac{\partial S}{\partial C} = \lim_{C \rightarrow \infty} \frac{\partial \left(\frac{\rho_b * a * b * C}{p * (1 + b * C)}\right)}{\partial C} = \lim_{C \rightarrow \infty} \frac{\rho_b * a * b}{p * (1 + b * C)^2} = 0 \quad (14)$$

The situation was the same for Sr. The adsorption capacity from the Langmuir isotherm was 0.39 Bq/g and $\Delta C = 60$ Bq/ml. This problem could be resolved by setting ΔC dependent on the current C value in the local model area. The solution was possible but complicated the problem significantly.

7. Results

Tab. 1. The simulation parameters and results according to the assumed scenario

Layer	WN-“dry” sands			WW-aquifer		
		Cs ¹³⁷	Sr ⁹⁰		Cs ¹³⁷	Sr ⁹⁰
Isotope	–	Cs ¹³⁷	Sr ⁹⁰	–	Cs ¹³⁷	Sr ⁹⁰
Decay constant (1/s)	–	7.30*10 ⁻¹⁰	7.62*10 ⁻¹⁰	–	7.30*10 ⁻¹⁰	7.62*10 ⁻¹⁰
Source	50000	50000	50000	50000	50000	50000
What is simulated	Advection, diffusion	Advection, diffusion, radioactive decay	Advection, diffusion, radioactive decay	Advection, diffusion	Advection, diffusion, radioactive decay	Advection, diffusion, radioactive decay
Diffusion coefficient (m ² /s)	10 ⁻⁹	10 ⁻⁹	10 ⁻⁹	10 ⁻⁹	10 ⁻⁹	10 ⁻⁹
Suction pressure (m) or Hydrological gradient	0.01	0.01	0.01	0.008	0.008	0.008
Advection velocity (m/s)	4.95*10 ⁻⁵	4.95*10 ⁻⁵	4.95*10 ⁻⁵	4.00*10 ⁻⁷	4.00*10 ⁻⁷	4.00*10 ⁻⁷
Spatial step (m)	2	2	2	20	20	20
Sum (ww)	49947	49896	49896	49941	17366	16557
Sum teor	50000	49991**	49991**	49947	17313**	16504**
Covergence	0.9989	0.9981	0.9981	0.9999	1	1
K – number of time steps	4700	5000	5000	1900	2900	2900
Δt – Time step (s)	50	50	50	500000	500000	500000
Simulated time	2.7 d	2.9 d	2.9 d	30 y	46 y***	46 y***
Time of simulation (s)	113	122	120	69	143	142
Peak value at the exudation (Bq/ml)	8257	8002	8002	4548	1280	1222

In the Table 1 simulation parameters for different scenarios are compared.

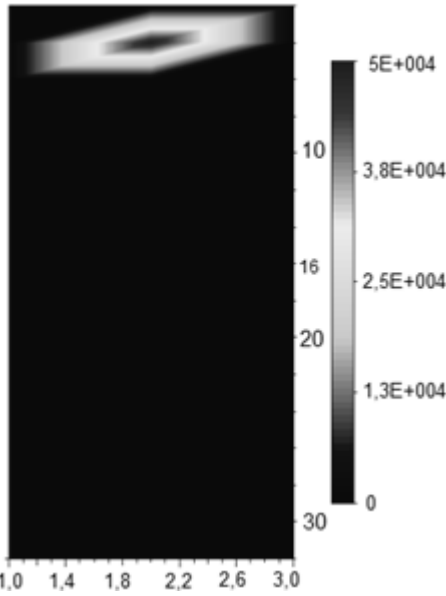
Figure 2 and 3 illustrate the contamination infiltration through the modeled area for the first case (model without radioactive decay): Scenario I, for the dry and hydrated sands, three time steps are shown as an example of a graphical solution of simulated problems.

* Sum (ww) is a sum of contaminant concentration in every knot when the simulation is completed. Sum (ww) for the WN layer is an input data to the WW layer.

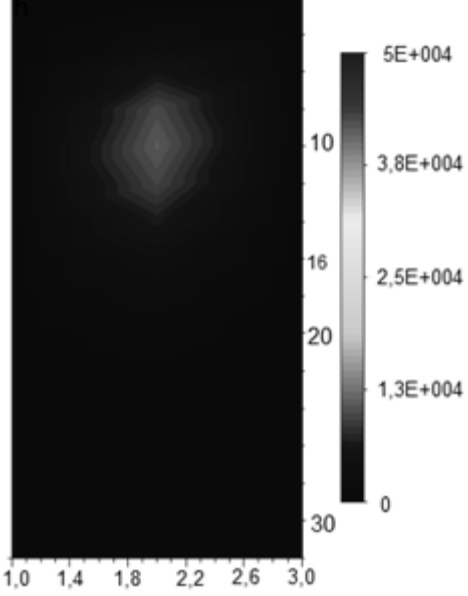
** Source multiplied by $\exp(-\lambda_{Cs,Sr} * \Delta t * k)$.

***After 30 years, the contamination peak reached the distance of 400 m, i.e. 66% of the distance from disposal to exudation.

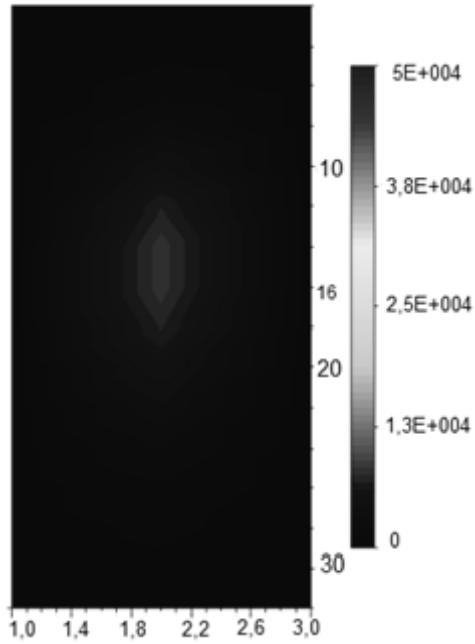
Scenario I - "dry" sands, time 0.04 h



Scenario I - "dry" sands, time 55 h



Scenario I - "dry" sands, time 98 h



Scenario I - "dry" sands, time 0.04 h, 55 h, 98 h

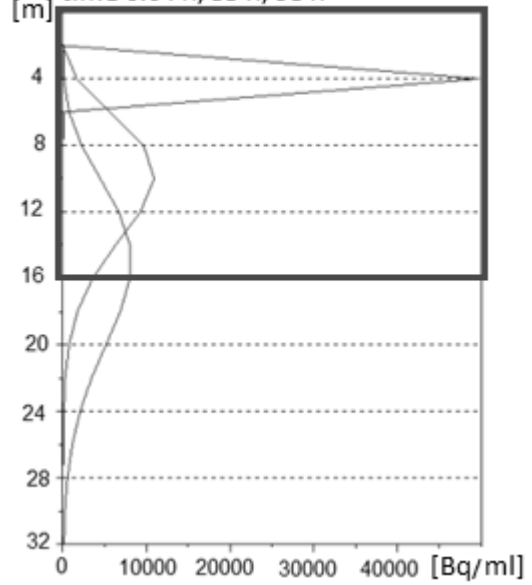


Fig. 2. Figures showing pollution propagation in the layer of "dry" sands in the time: 0.04 h, 55 h, 98 h, where $\Delta t = 50$ s. The distance of 16 m on the y axis – frame is an outflow

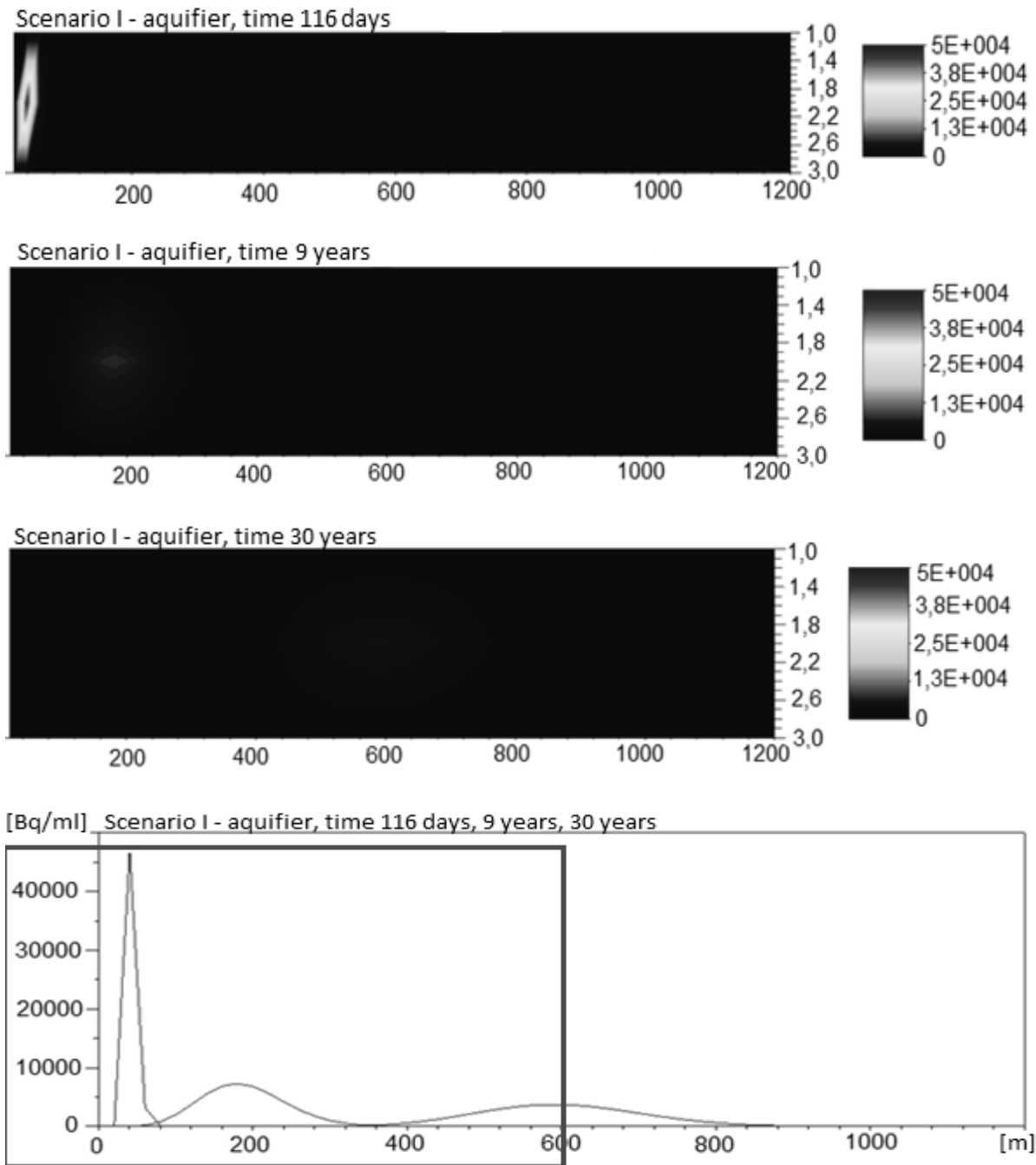


Fig. 3. Figures showing pollution propagation in the hydrated sands layer in time: 116 days, 9 years, 30 years, where $\Delta t = 500000$ s. The distance of 600 m on the x axis – frame means outflow

8. Discussion

As shown in Table 1, the simulations had very good convergence.

Testing the 8×3 grid for higher contamination values (10 times, 100 times, etc.) showed that the concentration distribution was not changed besides the decimal place shift. It can be assumed that for a higher source concentration value than the one defined in the model, the concentration distribution also would not change besides the decimal place

shift. That would allow the extrapolation of the results for higher source values.

Due to radiological protection, the peak concentration dispersion is very important. The higher the dispersion, the lower the exposition in the case of contact with exudation water.

The infiltration time of the peak concentration to the model edge differed in dependency on the assumed humidity for the dry sands and on the hydrological gradient for the hydrated sands. The distance from

the disposal bottom to the level of the hydrated sands is only about 16 m, and the infiltration time is about 3 days; in the context of decades, it is negligible. The infiltration time is important for the 600-m distance through the hydrated layer to Narew River.

Depending on the assumed scenario conditions, it is equal to 30 years for the advection–diffusion process and to 46 years for the advection–diffusion–radioactive decay process. Moreover, hydrological conditions influence the transportation time. The rain intensity differs between subsequent years, so the more valuable calculation of the infiltration time would require the use of archival data on the hydrological gradient on this area. Then a few more simulations can be performed and the weighted average could be calculated with respect to the rain intensity.

9. Conclusions

The simulator is a useful tool for simple engineering calculations, especially if the modeled area has a simple geometry. It is a sufficient alternative to commercially developed and expensive simulators. The available commercial products are relatively expensive in relation to the range of use.

The transportation equation can be used to simulate many physical problems, i.e. not only of concentration distribution but also for mass, charge, temperature and many others. This renders the simulator a universal tool.

According to the assumed parameters, the infiltration time of the contamination from below the bottom of the disposal to exudation in the Narew riverbank is 30–46 years.

The infiltration time through the dry sands layer is about 3 days. This time is very short on a century time scale, but it influences the pollution peak dispersion, which is meaningful because of radiological protection.

10. Founding source

This paper is a result of PhD dissertation survey implemented within the Human Capital Operational Program POKL.04.01.01-00-434/08-02, co-financed by the European Union.

11. Bibliography

- [1] Tomczak W., “Socioeconomic aspects in the development and operation of the national radioactive waste repository – Rozan”, in: *Low and Intermediate Level Waste Repositories: Socioeconomic Aspects and Public Involvement, Proceeding of a workshop held in Vienna, 9–11 November 2005*, IAEA TECDOC No. 1553, pp. 83–93, IAEA, Vienna 2007.
- [2] Objąsnienia do mapy hydrogeologicznej Polski w skali 1:50000. Arkusz Różan (372), Przedsiębiorstwo Geologiczne POLGEOL S.A., Państwowy Instytut Geologiczny, Warszawa 2002.
- [3] Widomski M., Kowalski D., Łagód G., *Modelowanie ruchu wody i transportu zanieczyszczeń w ośrodku porowatym: Przykłady zastosowania programu FEFLOW*, Lublin 2010.
- [4] Frankowski Z., Mitręga J., Tomczak W., *Badania monitoringowe Krajowego Składowiska Odpadów Promieniotwórczych w Różanie*, http://www.psh.gov.pl/plik/id.4680.v.artyku1_3312.pdf.
- [5] Berkowitz B., Dror I., Yaron B., *Contaminant geochemistry. Interactions and Transport in the Surface Environment*. Springer, Berlin 2008.
- [6] Trykozko A., “Modelowanie komputerowe w ochronie środowiska – wykład”, The Interdisciplinary Centre for Mathematical and Computational Modelling, University of Warsaw, <http://www.icm.edu.pl/~aniat> [access data: 19 November 2012].
- [7] da Silva F.E., “Paradoxes and difficulties associated to the use of nonlinear sorption isotherms on the numerical modeling of contaminant transport in groundwater”, <http://aguassubterraneas.abas.org/asubterraneas/article/view/23568/15646> [access data: 27 July 2015].
- [8] Tomczak W., “Krajowe składowisko odpadów promieniotwórczych w Różanie”, *Postępy Techniki Jądrowej*, Vol. 41, z. 4 (1998).
- [9] Ahn J., Apted M.J. (eds), *Geological repository systems for safe disposal of spent nuclear fuels and radioactive waste*, Woodhead Publishing Series in Energy, 2010.

12. Supplementary data

SciLab code: Dry Sands layer

```
clear
clc
stacksize('max')//the function maximizing the stack size - there is no
limitation of variable size
tic();//starting the simulation time measurement
function b=fprintMatAppend(filename, data)//the function to write and
read data to and from text files copied from:
www.equalis.com/forums/Posts.aspx?topic=328521
if isfile(filename) then
    txt = mgetl(filename);
else
```

```

txt = [];
end
fprintfMat(TMPDIR + "/Mat", data);
txt = [txt;mgetl(TMPDIR + "/Mat")];
b = mputl(txt, filename);
endfunction//the end of the function writing and reading data to and from the
text file
z=zeros(16,3);//defining the model size
x=1:1:size(z,2);//vector defining the number of columns in the model
y=1:1:size(z,1);//vector defining the number of verses in the model
v1=0;//the advection velocity on model boundaries sides and upper
H1=0;//the diffusion coefficient on model boundaries sides and upper
vx=0;//the advection velocity in the x direction - horizontal
Hx=0;//the diffusion coefficient in the x direction - horizontal
wf=5*10^-5;//the filtration coefficient
h=0.01;//the suction pressure expressed in [m]
vy=wf*(1-h);//the advection velocity in the y direction - vertical
Hy=1*10^-9;//the diffusion coefficient in the y direction - vertical (m^2/s)
dy=2;//the spatial step in the y direction - vertical
dx=2;//the spatial step in the x direction - horizontal
dt=50;//the time step
lambda=0//7.63*10^-10;//the radioactive decay constant for Cs-137
w=z;//the calculation matrix
w(2,2)=50000;//the source definition
aL=0/580;//Langmuir isotherm parameter
bL=0/0.0035;//Langmuir isotherm paramet
dC=30000;//the concentration step
show_window();clf();//functions opening the graphic window and cleaning
the graphic window
f=getf();
f.color_map=jetcolormap(64);//setting the graphic colours
//f.pixmap='on';
colorbar(0,50000)//the caption definition
Sgrayplot(y,x,z,strt="081",zminmax=[0,50000])//setting the graphic colour
to changing values of results
a=gca();
a.rotation_angles=[0 360];
c=gce(),e=c.children
xtitle("Równanie transportu bez adsorpcji-Scenariusz IV")//the graphic title
//dijfinig parameters
A=1/dt-v1/dy-v1/dx+2*H1/dy^2+2*H1/dx^2;
A1=1/dt-v1/dy+v1/dx+2*H1/dy^2+2*H1/dx^2;
A2=1/dt+vy/dy-vx/dx+2*Hy/dy^2+2*Hx/dx^2;
A3=1/dt+vy/dy+vx/dx+2*Hy/dy^2+2*Hx/dx^2;
A31=1/dt+v1/dy+v1/dx+2*H1/dy^2+2*H1/dx^2;
A21=1/dt+v1/dy-v1/dx+2*H1/dy^2+2*H1/dx^2;
L=-vy/dy-Hy/dy^2;
L1=-v1/dy-H1/dy^2;//left boundary
C=-Hy/dy^2;
C1=-H1/dy^2;
L2=-vx/dx-Hx/dx^2;
L21=-v1/dx-H1/dx^2;//top and bottom boundary
E=-Hx/dx^2;
E1=-H1/dx^2;//top and bottom boundary
F=v1/dx-2*H1/dx^2;//left boundary
I=-v1/dx-2*H1/dx^2;//right boundary
J=-vy/dy-2*Hy/dy^2;//bottom
B=v1/dy-2*H1/dy^2;//top
D=zeros(max(x)*max(y),max(x)*max(y));//defining the matrix of
parameters
//filling the matrix of parameters
D=eye(D).*A3+diag(ones(max(x)*(max(y)-1),1)*L,-
max(x))+diag(ones(max(x)*(max(y)-
1),1)*C,max(x))+diag(ones(max(x)*(max(y)-1),1)*L2,-
1)+diag(ones(max(x)*(max(y)-1),1)*E,1);
for i=1+max(x)*max(y)-max(x):max(x)*max(y)
D(i,i)=A31;
end
for i=2*max(x):max(x):max(x)*max(y)-max(x)
D(i,i)=A31;//the right boundary
end
for i=1:max(x)
D(i,i)=A1;
end
D(1,1)=A;
for i=-max(x)+1:max(x):max(x)*max(y)
D(i,i)=A21;
end
for i=1+max(x)*max(y)-2*max(x):max(x)*max(y)-max(x)
D(i+max(x),i)=J;
end
for i=1:max(x)
D(i,i+max(x))=B;
end
for i=-max(x):max(x):max(x)*max(y)
D(i,i-1)=I;
end
for i=-max(x):max(x):max(x)*(max(y)-1)
D(i+1,i)=0;
end
for i=1:max(x):max(x)*max(y)
D(i,i+1)=F;
end
//replacing E on the top
for i=2:max(x)-1
D(i,i+1)=E1;
end
//replacing L on the top
for i=1:max(x)-2
D(i+1,i)=L21;
end
//replacing L on the bottom
for i=1+max(x)*max(y)-max(x):max(x)*max(y)-2
D(i+1,i)=L21;
end
//replacing L on right
for i=1:max(x):max(x)*max(y)-max(x)
D(i+1,i)=L21;
end
//replacing E on the bottom
for i=2+max(x)*max(y)-max(x):max(x)*max(y)-1
D(i,i+1)=E1;
end
//replacing L in i,1
for i=1:max(x):max(x)*max(y)-max(x)
D(i+max(x),i)=L1;
end
//replacing C in i,1
for i=1+max(x):max(x):max(x)*max(y)-max(x)
D(i,i+max(x))=C1;
end
//replacing L on the right side
for i=-max(x):max(x):max(x)*max(y)-2*max(x)
D(i+max(x),i)=L1;
end
//replacing C on the right
for i=2*max(x):max(x):max(x)*max(y)-max(x)
D(i,i+max(x))=C1;
end
for i=-max(x):max(x):max(x)*(max(y)-1)
D(i,i+1)=0;
end
for k=1:1:4700
S1=aL*bL*w./(1+bL*w);//calculating the isotherm
S2=aL*bL*(w+dC)/(1+bL*(w+dC));//calculating the isotherm
R=1+(S2-S1)/dC;//calculating the isotherm
R1=[R(1,:) R(2,:) R(3,:) R(4,:) R(5,:) R(6,:) R(7,:) R(8,:) R(9,:) R(10,:)
R(11,:) R(12,:) R(13,:) R(14,:) R(15,:) R(16,:)];//defining the matrix of
retardation factor
//multiplying the diagonal of the parameters matrix by the retardation
factor
for i=1:max(x)*max(y)
D(i,i)=R1(1,i)/dt+vy/dy+vx/dx+2*Hy/dy^2+2*Hx/dx^2//A3
end
for i=1:max(x):max(x)*max(y)
D(i,i)=R1(1,i)/dt+vy/dy-vx/dx+2*Hy/dy^2+2*Hx/dx^2//A2
end
for i=1:max(x)
D(i,i)=R1(1,i)/dt-vy/dy+vx/dx+2*Hy/dy^2+2*Hx/dx^2//A1
end
D(1,1)=R1(1,1)/dt-vy/dy-vx/dx+2*Hy/dy^2+2*Hx/dx^2;
for i=1:max(y)//defining the matrix of known based on the initial
conditions or the previous calculation step
for j=1:max(x)
Z((i-1)*max(x)+j)=(-w(i+max(y)*(k-1),j)/dt*exp(-lambda*dt))/in
this place the radioactive decay is included
end
end
Z1=R1.*Z;//multiplying the matrix of known by the retardation factor
X=insolve(D,Z1);//the SciLab function solving the linear system of
equations - at this place there can be used the iteration method of solving the
linear system of equations numericaly
for j=1:max(y)
for i=1:max(x)
w(i+max(y)*k,j)=X(j+max(x)*(i-1),1);//saving the solution to the
matrix of calculation matrix
end
end
ww=w(1+max(y)*k:max(y)+max(y)*k,:);//saving the last time step results
e.data(:,3)=matrix(ww,-1,1);//ploting the last time step in the graphical
window
// show_pixmap()
for j=1:max(y);
Q(k,j)=w(max(y)*(k-1)+j,2);//saving the middle column as a 1D result
the two other columns are equal to 0
end
fprintfMatAppend('k:QWN.txt', Q(k,:))//saving the result to the text flie
end
//f.pixmap='off';

```

```
fprintfMatAppend('k:\QWN.txt', Q(max(k,:)))/saving the result to the text
file in this case that was a memory stick
t2=toc();/switching off the timer
```

SciLab code – hydrated sands layer – aquifer

```
clear
clc
stacksize('max')/the funkcjon maximizing the stack size - there is no
limitation of variable size
tic()/starting the simulation time measurement
function b=fprintfMatAppend(filename, data)/the function to write and
read data to and from text files copied from:
www.equalis.com/forums/Posts.aspx?topic=328521
if isfile(filename) then
    txt = mgetl(filename);
else
    txt = [];
end
fprintfMat(TMPDIR + "/Mat", data);
txt = [txt;mgetl(TMPDIR + "/Mat")];
b = mputl(txt, filename);
endfunction/the end of the function writing and reading data from to and
from the text file
z=zeros(3,60)/defining the model size
x=1:1:size(z,2)/vector defining the number of columns in the model
y=1:1:size(z,1)/vector defining the number of verses in the model
QWN=mgetl('k:\QWN.txt')/reading the results of the WN simulation when
the maximum concentration peak reaches the vertical (WN) model boundary
in this case from the memory stick
QWN=evstr(QWN)/changing the format from string to double:
https://groups.google.com/forum/#!topic/comp.soft-sys.math.scilab/B-
pG3pdhp58
for i=1:16/inversion of the data from the text file-this that was first
outflowing now will be first inflowing
    QWNR(i)=QWN(17-i);
end
v1=0;/the advection velocity on model boundaries sides and upper
H1=0;/the diffusion coefficient on model boundaries sides and upper
vy=0;/the advection velocity in the y direction - vertical
Hy=0;/the diffusion coefficient in the y direction - vertical(m^2/s)
wf=5*10^-5;/the filtration coefficient
grad_h=0.008;/hydrological gradient
vx=wf*grad_h;/the advection velocity in the x direction - horizontal
Hx=1*10^-9;/the diffusion coefficient in the x direction - horizontal
lambda=0/7.63*10^-10;/the radioactive decay constant for Cs-137
w=z;/the calculation matrix
dy=10;/the spatial step in the y direction - vertical
dx=20;/the spatial step in the x direction - horizontal
dt=500000;/the time step
aL=0/580/Langmuir isotherm parameter
bL=0/0.0035/Langmuir isotherm parameter
dC=30000;/the concentration step
show_window();clf()/functions opening the graphic window and cleaning
the graphic window
f=gcf();
f.color_map=jetcolormap(64)/setting the graphic colours
/f.pixmap='on';
colorbar(0,50000)/the caption definition
Sgrayplot(y,x,z,strf="081",zminmax=[0,50000])/setting the graphic colour
to changing values of results
a=gca();
a.rotation_angles=[0 360];
c=gce(),e=c.children
xtitle("R6wnanie transportu bez adsorpcji-Scenariusz I")/the graphic title
//defining parameters
A=1/dt-v1/dy-v1/dx+2*H1/dy^2+2*H1/dx^2;
A1=1/dt-v1/dy+v1/dx+2*H1/dy^2+2*H1/dx^2;
A2=1/dt+vy/dy-vx/dx+2*Hy/dy^2+2*Hx/dx^2;
A3=1/dt+vy/dy+vx/dx+2*Hy/dy^2+2*Hx/dx^2;
A31=1/dt+v1/dy+v1/dx+2*H1/dy^2+2*H1/dx^2;
A21=1/dt+v1/dy-v1/dx+2*H1/dy^2+2*H1/dx^2;
L=-vy/dy-Hy/dy^2;
L1=-v1/dy-H1/dy^2;/left boundary
C=-Hy/dy^2;
C1=-H1/dy^2;
L2=-vx/dx-Hx/dx^2;
L21=-v1/dx-H1/dx^2;/top and bottom boundary
E=-Hx/dx^2;
E1=-H1/dx^2;/top and bottom boundary
F=v1/dx-2*H1/dx^2;/left boundary
I=-v1/dx-2*H1/dx^2;/right boundary
J=-v1/dy-2*H1/dy^2;/bottom
B=v1/dy-2*H1/dy^2;/top
D=zeros(max(x)*max(y),max(x)*max(y))/defining the matrix of
parameters
//filling the matrix of parameters
D=eye(D).*A3+diag(ones(max(x)*(max(y)-1),1)*L,-
max(x))+diag(ones(max(x)*(max(y)-
1),1)*C,max(x))+diag(ones(max(x)*max(y)-1,1)*L2,-
1)+diag(ones(max(x)*max(y)-1,1)*E,1);
for i=1+max(x)*max(y)-max(x):max(x)*max(y)
    D(i,i)=A31;
end
for i=2*max(x):max(x):max(x)*max(y)-max(x)
    D(i,i)=A31;/the right boundary
end
for i=1:max(x)
    D(i,i)=A1;
end
D(1,1)=A;
for i=max(x)+1:max(x):max(x)*max(y)
    D(i,i)=A21;
end
for i=1+max(x)*max(y)-2*max(x):max(x)*max(y)-max(x)
    D(i+max(x),i)=J;
end
for i=1:max(x)
    D(i+max(x))=B;
end
for i=max(x):max(x):max(x)*max(y)
    D(i,i-1)=I;
end
for i=max(x):max(x):max(x)*(max(y)-1)
    D(i+1,i)=0;
end
for i=1:max(x):max(x)*max(y)
    D(i,i+1)=F;
end
//replacing E on the top
for i=2:max(x)-1
    D(i,i+1)=E1;
end
//replacing L on the top
for i=1:max(x)-2
    D(i+1,i)=L21;
end
//replacing L on the bottom
for i=1+max(x)*max(y)-max(x):max(x)*max(y)-2
    D(i+1,i)=L21;
end
//replacing L on right
for i=1:max(x):max(x)*max(y)-max(x)
    D(i+1,i)=L21;
end
//replacing E on the bottom
for i=2+max(x)*max(y)-max(x):max(x)*max(y)-1
    D(i,i+1)=E1;
end
//replacing L in i,1
for i=1:max(x):max(x)*max(y)-max(x)
    D(i+max(x),i)=L1;
end
//replacing C in i,1
for i=1+max(x):max(x):max(x)*max(y)-max(x)
    D(i,i+max(x))=C1;
end
//replacing L on the right side
for i=max(x):max(x):max(x)*max(y)-2*max(x)
    D(i+max(x),i)=L1;
end
//replacing C on the right
for i=2*max(x):max(x):max(x)*max(y)-max(x)
    D(i,i+max(x))=C1;
end
for i=max(x):max(x):max(x)*(max(y)-1)
    D(i,i+1)=0;
end
for k=1:1:1900
    if k<17 then/the part of the calculations that is executed when the inflow
    is defined
        S1=aL*bL*w./(1+bL*w)/calculating the isotherm
        S2=aL*bL*(w+dC)/(1+bL*(w+dC))/calculating the isotherm
        R=1+(S2-S1)/dC;/calculating the isotherm
        R1=[R(1,:); R(2,:); R(3,:)]/defining the matrix of retardation factor
        //multiplying the diagonal of the parameters matrix by the
        retardation factor
        for i=1:max(x)*max(y)
            D(i,i)=R1(1,i)/dt+vy/dy+vx/dx+2*Hy/dy^2+2*Hx/dx^2;/A3
        end
        for i=1:max(x):max(x)*max(y)
            D(i,i)=R1(1,i)/dt+vy/dy-vx/dx+2*Hy/dy^2+2*Hx/dx^2;/A2
        end
        for i=1:max(x)
            D(i,i)=R1(1,i)/dt-vy/dy+vx/dx+2*Hy/dy^2+2*Hx/dx^2;/A1
        end
        D(1,1)=R1(1,1)/dt-vy/dy-vx/dx+2*Hy/dy^2+2*Hx/dx^2;
```

```

for i=1:max(y)//defining the matrix of known based on the initial
conditions or the previous calculation step
for j=1:max(x)
Z((i-1)*max(x)+j)=-w(i+max(y)*(k-1),j)/dt*exp(-
lambda*dt)//in this place the radioactive decay is included
end
end
Z(max(x)+2)=Z(max(x)+2)-QWNR(k)/dt//subtraction the inflow
from the matrix of known
Z1=R1.*Z;//multiplying the matrix of known by the retardation
factor
X=linsolve(D,Z1);//the SciLab function solving the linear equations
system
for i=1:max(y)
for j=1:max(x)
w(i+max(y)*k,j)=X(j+max(x)*(i-1),1)//writings the resoult to
the calculation matrix
end
end
ww=w(1+max(y)*k:max(y)+max(y)*k,;)//writing the last
calculation step
e.data(:,3)=matrix(ww,-1,1);//printing the last calculation step in the
graphic window
// show_pixmap()
for j=1:max(x)
Q(k+1,j)=w(3*k+2,j)//writing the middle column of the calculating
matrix as a result, other elements are equal zero
end
else//the part of the program that starts when ther is no more inflow
S1=aL*bL*w./(1+bL*w);
S2=aL*bL*(w+dC)/(1+bL*(w+dC));
R=1+(S2-S1)/dC;
R1=[R(1,:) R(2,:) R(3,:)];
for i=1:max(x)*max(y)
D(i,i)=R1(1,i)/dt+vy/dy+vx/dx+2*Hy/dy^2+2*Hx/dx^2//A3
end
for i=1:max(x):max(x)*max(y)
D(i,i)=R1(1,i)/dt+vy/dy-vx/dx+2*Hy/dy^2+2*Hx/dx^2//A2
end
for i=1:max(x)
D(i,i)=R1(1,i)/dt-vy/dy+vx/dx+2*Hy/dy^2+2*Hx/dx^2//A1
end
D(1,1)=R1(1,1)/dt-vy/dy-vx/dx+2*Hy/dy^2+2*Hx/dx^2;
for i=1:max(y)
for j=1:max(x)
Z((i-1)*max(x)+j)=-w(i+max(y)*(k-1),j)/dt*exp(-
lambda*dt)//!!!!!!
end
end
Z(max(x)+2)=Z(max(x)+2);
Z1=R1.*Z;
X=linsolve(D,Z1);
for i=1:max(y)
for j=1:max(x)
w(i+max(y)*k,j)=X(j+max(x)*(i-1),1);
end
end
ww=w(1+max(y)*k:max(y)+max(y)*k,;);
e.data(:,3)=matrix(ww,-1,1);
// show_pixmap()
for j=1:max(x)
Q(k+1,j)=w(3*k+2,j)
end
// fprintfMatAppend('k:\QWW3.txt', Q(k))//writing the result to the
text file
end
end
//f.pixmap='off';
t2=toc();//schwitchnig off the timer

```

Modelownie procesu transportu Cs¹³⁷ i Sr⁹⁰ w okolicy Krajowego Składowiska Odpadów Promieniotwórczych w Różanie (północno-wschodnia Polska)

M. MIECZNIK, J.W. MIETELSKI, E. ŁOKAS, K. KLESZCZ

Artykuł zawiera wyniki modelowania transportu potencjalnego skażenia Cs¹³⁷ i Sr⁹⁰, przeprowadzonego dla wód podziemnych pod Krajowym Składowiskiem Odpadów Promieniotwórczych w Różanie (północno-wschodnia Polska). KSOP jest składowiskiem odpadów nisko- i średnioaktywnych. Modelowanie zostało przeprowadzone w samodzielnie napisanym symulatorze, w programie SciLab, z wykorzystaniem metody różnic skończonych. Symulowano proces transportu radionuklidów przez piaszczyste gleby. Model zawierał dyfuzję, adwekcję i rozpad promieniotwórczy. Model został przetestowany pod względem zbieżności i stabilności. Modelowany czas transportu skażeń spod dna składowiska do koryta rzeki Narew, przy założeniu gradientu hydrologicznego 0.008, wynosił od 30 do 46 lat w zależności od przyjętego scenariusza. Modelowany dystans wynosił 600 m. Rozpad promieniotwórczy miał znaczący wpływ na uzyskane rezultaty. Modelowanie potwierdziło, że symulator jest użytecznym narzędziem do przeprowadzania prostych, naukowych symulacji. Przeprowadzone badania były częścią pracy doktorskiej.

Słowa kluczowe: adwekcja, dyfuzja, rozpad promieniotwórczy.